EFFECT OF OIL DEGASSING IN A BED ON THE PROGRESS OF HYDRODYNAMIC PROCESSES IN A "CONNECTING PIPE–WELL-BED" SYSTEM

S. D. Tseitlin

UDC 532.546

Using a numerical dynamic model of the connecting pipe–well-bed system, the effect of oil degassing in a bed on the progress of hydrodynamic processes in oil has been analyzed by the method of successive steady states.

Introduction. Because of the depletion of oil deposits with productive relatively shallow beds that are simple intergranular reservoirs, a compelling need arises for a comprehensive investigation of hydrodynamic processes occurring in composite beds saturated with a multiphase fluid. Many of the techniques of prospecting and developing oil deposits, which are based on the solution of relatively simple hydrodynamic problems and usually employed in the work with porous reservoirs, do not ensure sufficient accuracy when used for hydrodynamic testing of composite beds. The invention of more complex adequate mathematical models is needed to study hydrodynamic processes in a connecting pipe–well-bed system which would allow one to develop interpretation procedures and equipment to provide higher accuracy when conducting hydrodynamic testing of composite beds.

In [1] the statement and solution are given for the problem which describes the dynamics of a connecting pipe–well-bed systems taking account of the composite (including fissured) pattern of the bed and the two-phase nature of the fluid flowing through tubing strings (TS) and connecting pipe. Consideration of the connecting pipe–well bed system in such a context can also be useful for solving practical problems on the increase of oil recovery from composite reservoirs.

It should be noted that the degassing of oil in a bed, as practice has shown, complicates interpretation of the results of hydrodynamic tests and also entails a decrease in oil recovery from it. Below, an analysis of the effect of oil degassing in a bed on the occurrence of processes in a connecting pipe–well-bed system is given which is based on the numerical model of the process described in [1].

Statement of the Problem. In [2, 3], a system of equations has been derived that describe nonsteady-state multicomponent filtration in oil-bearing beds. In particular, their form for a gasified liquid is given. Further, it will be assumed throughout that the liquid is oil and the gas is the casing-head gas which can be in a free state or dissolved in oil.

In general, pressure in oil P_{oil} differs from pressure in gas P_g because of the presence of capillary properties ($P_{oil} - P_g = P_{cap}(\sigma_{oil})$). However, numerical solution, which takes into account this phemonenon [4], shows that in the majority of cases this pressure does not virtually exert any effect on the results and therefore we assume that $P_{oil} = P_g = P$ throughout.

The simultaneous equations for this case are [2]

$$\operatorname{div}\left[\left(\frac{\bar{k}_{oil}\rho_{g\,0}S}{\mu_{oil}\beta_{oil}} + \frac{\bar{k}_g\rho_g}{\mu_g}\right)\operatorname{grad}P\right] = \frac{m}{k}\frac{\partial}{\partial t}\left(\frac{\sigma_{oil}\rho_{g\,0}S}{\beta_{oil}} + \rho_g(1-\sigma_{oil})\right),$$
$$\operatorname{div}\left(\frac{\bar{k}_{oil}}{\mu_{oil}\beta_{oil}}\operatorname{grad}P\right) = \frac{m}{k}\frac{\partial}{\partial t}\left(\frac{\sigma_{oil}}{\beta_{oil}}\right). \quad (1)$$

All of these parameters are functions of the pressure P (here we assume the processes to be isothermal, i.e., T = const); σ_{oil} and P, the oil saturation and pressure, are the unknown functions.

Central Geophysical Expedition, Moscow. Translated from Inzhenerno-Fizicheskii Zhurnal, Vol. 63, No. 1, pp. 3-10, July, 1992. Original article submitted March 25, 1991.

We know that the gas factor Γ_g is the ratio between the volumetric flow rate of gas, reduced to atmospheric pressure Q_{g0}, and the volumetric flow rate of oil Q_{oil0} through a unit section: $\Gamma_g = Q_{g0}/Q_{oil0}$, where

$$Q_{g0} = \frac{(\rho_g v_g)_0}{\rho_{g0}} \omega = \left(\frac{\rho_g}{\rho_{g0}} v_g + \frac{S}{\beta_{oil}} v_{oil}\right)\omega;\ Q_{oil0} = \frac{\rho_{oil} v_{oil}}{\beta_{oil0}} \omega = \frac{v_{oil}}{\beta_{oil}} \omega;$$

$(\rho_g v_g)_0$ is the overall gas velocity.

Taking into account the expression for filtration velocities (Darcy law) [2]

$$v_j = -\frac{k_j}{\mu_j} \bar{k}_j(\sigma_j) \frac{\partial P}{\partial x}, \quad j = \text{г, н}, \tag{2}$$

we obtain

$$\Gamma_g = \frac{\rho_g(P) v_g \beta_{oil}(P)}{\rho_{g0} v_{oil}} + S(P) = \frac{\rho_g(P) \beta_{oil}(P) k_g / k_{oil}}{\rho_{g0} \mu_g(P)/\mu_{oil}(P)} + S(P). \tag{3}$$

It is shown in [2, 3] that for a steady-state flow of a gasified liquid along streamlines Γ_g = const, i.e.,

$$\frac{\rho_g(P) \beta_{oil}(P)}{\rho_{g0} \dfrac{\mu_g(P)}{\mu_{oil}(P)}} \frac{k_g(\sigma_{oil})}{k_{oil}(\sigma_{oil})} + S(P) = \Gamma_{g0} = \text{const}. \tag{4}$$

For approximate calculations of gasified liquid flow in beds, use is often made of the method of successive steady states [2, 5]. In such cases it is important, for example, to solve the filtration equation for unsteady single-component filtration taking into account the change in the permeability coefficients derived from Eq. (4). Such an approach, which is valid for relatively slow processes, considerably simplifies the solution of the problem posed and does not incur large errors in the solution results, as is evident from comparison of exact solutions based on Eqs. (1) [3, 4] with approximate ones.

The method as such is realized in the following way. Assuming that the gas factor along streamlines varies little for a certain period of time ($\Gamma_g = \Gamma_{g0}$ = const) and knowing the functions $k_g(P)$ and $k_{oil}(P)$ (for example, [3, 5]), and also the functions $\beta_{oil}(P)$, $\rho_g(P)$, $\rho_g(P)$, $\rho_{oil}(P)$, S(P), $\mu_g(P)$, $\mu_{oil}(P)$, we find first the relationship between the oil saturation and pressure and then the dependence of the relative permeability on pressure $k_{oil} = k_p(P)$ from Eq. (4). We shall consider as an example the case when $\Gamma_g = \Gamma_{g0}$ = const, $\rho_g = \rho_{g0} P/P_{atm}$, $S(P) = SP/P_{atm}$, β_{oil} = const, and $\mu_g/\mu_{oil} = \mu_0$ = const. Then Eq. (4) is of the form

$$\frac{P}{P_{atm}} \frac{k_g}{k_{oil}} \frac{\mu_{oil}}{\mu_g} + S \frac{P}{P_{atm}} = \Gamma_{g0} = \text{const}. \tag{5}$$

Whence

$$\frac{k_g}{k_{oil}} = \left(\frac{\Gamma_{g0} P_{atm}}{P} - S\right) \frac{\mu_g}{\mu_{oil}},$$

or

$$\frac{k_g}{k_{oil}} = \frac{\Gamma_{g0}}{P^*} - \alpha, \tag{6}$$

where

$$P^* = \frac{P \mu_{oil}}{P_{atm} \mu_g}; \quad \alpha = S \frac{\mu_g}{\mu_{oil}}.$$

The characteristic form of phase permeabilities for the most abundant types of reservoirs is given in [2-5]. It is obtained by laboratory measurements. In particular, in [3, 4] one of the versions of their analytical representation is given:

$$\bar{k}_{oil}(\sigma_{oil}) = 1{,}06\sigma_{oil}^3 - 0{,}06 \simeq \sigma_{oil}^3, \bar{k}_g(\sigma_{oil}) = 1{,}16(1 - \sigma_{oil}^2) \simeq (1 - \sigma_{oil}^2). \tag{7}$$

A comparison of the relations obtained experimentally [3] with those calculated from Eq. (7) displays their good agreement.

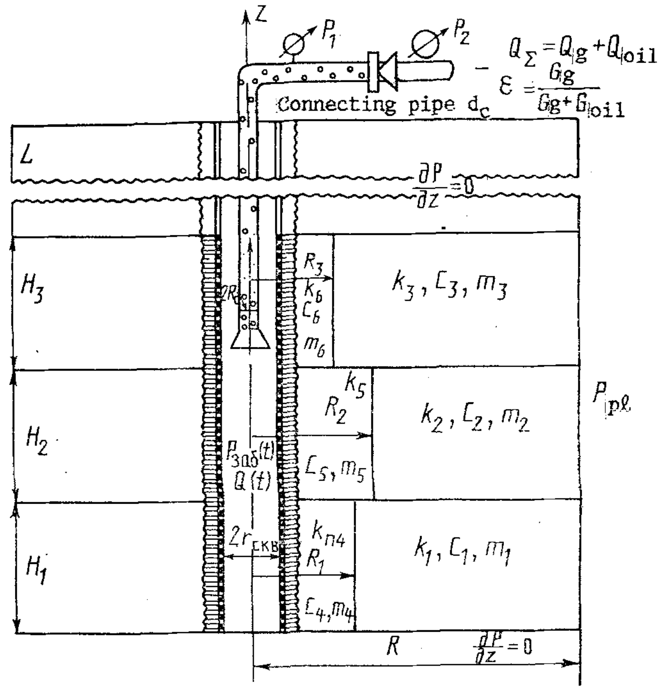

Fig. 1. General view of the model at hand.

It follows from the relations for phase permeabilities given in [2-5] that it is possible to find an approximate analytical relationship between k_{oil} and P for oil saturations close to unity on the basis of Eqs. (4) and (7).

In fact, according to (7) and taking into account the fact that $\sigma_{oil} \approx 1$, we obtain

$$\frac{k_g}{k_{oil}} = \frac{(1-\sigma_{oil})^2}{\sigma_{oil}^3} = \left(\frac{1-\sigma_{oil}}{\sigma_{oil}}\right)^2 \frac{1}{\sigma_{oil}} \simeq \left(\frac{1-\sigma_{oil}}{\sigma_{oil}}\right)^2;$$

then, according to (4),

$$\frac{k_g}{k_{oil}} = \left(\frac{1}{\sigma_{oil}} - 1\right)^2 = \left(\frac{\Gamma_g P_{atm}}{P} - S\right)\frac{\mu_g}{\mu_{oil}} = \frac{1}{P^*} - \alpha$$

or

$$\sigma_{oil} = \left[1 + \sqrt{\left(\frac{\Gamma_g P_{atm}}{P} - S\right)\frac{\mu_g}{\mu_{oil}}}\right]^{-1}$$

and finally

$$\bar{k}_{oil}(P^*) \simeq \sigma_{oil}^3 = \left[1 + \sqrt{\frac{1}{P^*} - \alpha}\right]^{-3} \qquad (8)$$

A comparison was carried out between the function $\bar{k}_{oil}(P^*)$ from [5] and the functions calculated from Eq. (8) for α = 0.01 and 0.02. It revealed that analytical expression (8) with a good approximates the dependence obtained numerically from (4) for averaged characteristic functions $k_g(\sigma_{oil})$ and $k_{oil}(\sigma_{oil})$ from [5] with a good accuracy (~15%).

For further studies we shall borrow from [1] the system of differential equations and the algorithm that describe the dynamics of the connecting pipe–well-bed system and that allow one to take into account the dependence of the permeability on the instantaneous pressure in a bed, including also the case of the dependence of form (8).

Thus, we shall formulate the problem set. A mathematical model of the connecting pipe–well-bed system consists (see Fig. 1) of a model for the bed involving three interlayers of thickness H_1, H_2, and H_3 with the reservoir properties k_i, m_i, and C_i (i = 1, 2, 3). The middle, relatively thin layer ($H_2 < \{H_1, H_3\}$) has higher permeability ($k_2 > \{k_1, k_3\}$). The layers were perforated by a well of radius r_w. Each of the layers may have the near-well zone of radius R_j with altered reservoir properties k_j, m_j, and C_j (j = 4, 5, 6).

In a cylindrical coordinate system, the equation which describes the process of nonsteady-state filtration of a homogeneous liquid in such a bed can be obtained from a system of equations (1); it has the form

$$m_i C_i \mu_{oil} \frac{\partial P}{\partial t} = \frac{1}{r} \frac{\partial}{\partial r} \left(r k_i (P) \frac{\partial P}{\partial r} \right) + \frac{\partial}{\partial z} \left(k_i (P) \frac{\partial P}{\partial z} \right), \tag{9}$$

$$i = 1, 2, \ldots, 6;$$

$$k_i (P) = k_{io} \left[1 + \sqrt{\frac{1}{P^*} - \alpha} \right]^{-3} \tag{10}$$

is the function of pressure, it depends on the gas number Γ_g, gas solubility S, and on the viscosities of gas μ_g and oil μ_{oil}.

Equation (9) is augmented with boundary-value conditions on the outer and inner boundaries of the region

$$\begin{gathered} \frac{\partial P}{\partial z}(r, z = 0, t) = \frac{\partial P}{\partial z}(r, z = H, t) = 0, \\ P_i (r, z = H_i, t) = P_{i+1} (r, z = H_i, t), \\ Q_i (r, z = H_i, t) = Q_{i+1} (r, z = H_i, t). \end{gathered} \tag{11}$$

At the boundary representing the surface of the well the solution agrees, with respect to the pressure and flow rate, with that obtained with the help of the one-dimensional two-phase pipe flow model [1]:

$$\begin{gathered} \frac{\partial P}{\partial z} = \varphi \rho_g + (1 - \varphi) \rho_{oil} + \frac{\lambda}{2Dg} [\varphi \rho_g v_g^2 + (1 - \varphi) \rho_{oil} v_{oil}^2]; \\ \frac{\pi}{4} \varphi D^2 \rho_g g v_g = Q_g \rho_g g = G_g = \text{const}; \\ \frac{\pi}{4} (1 - \varphi) D^2 \rho_{oil} g v_{oil} = Q_{oil} \rho_{oil} g = G_{oil} = \text{const}, \end{gathered} \tag{12}$$

where λ is the hydraulic drag coefficient which depends on $Re = vD\rho/\mu$.

For a homogeneous flow ($v_g = v_{oil}$) the volumetric gas content is

$$\varphi = \frac{Q_g}{Q_g + Q_{oil}}.$$

The pressure and flow rate in the upper cross section of the pipe (at the mouth of the well) agree with the solution obtained with the help of the connecting pipe model [1] which allows one to calculate the homogeneous gas–liquid mixture flow through a diffuser for any inlet P_1 to outlet P_2 pressure ratios:

$$f = (G_g + G_{oil}) [M (\varkappa^{2/\xi} - \varkappa^{(\xi+1)/\xi}) + k (\varkappa^{2/\xi} - \varkappa^{(2+\xi)/\xi})]^{-\frac{1}{2}}, \tag{13}$$

where f is the flow area of the connecting pipe

$$\varkappa = P_2/P_1; \quad \xi = \frac{\eta c_p + c_{oil}}{\eta c_v + c_{oil}}; \quad \eta = \frac{G_g}{G_{oil}};$$

$$M = \tilde{c}^2 \frac{2\xi}{\xi - 1} \frac{1 + \eta}{\eta} \rho_{oil} \frac{P_1}{P_2}; \quad k = \frac{2\tilde{c}^2 \rho_g^2 \rho_1^2}{\rho_{oil} P_2^2} \frac{1 + \eta}{2};$$

$\tilde{c}$ is the connecting pipe factor.

The numerical algorithm for the problem [1] allows one to obtain the pressure distribution and fluid flow rate throughout the entire connecting pipe–well-bed system at any time instant depending on the diameter of the connecting pipe, pressure downstream of it and in the bed, and also on other parameters of the system.

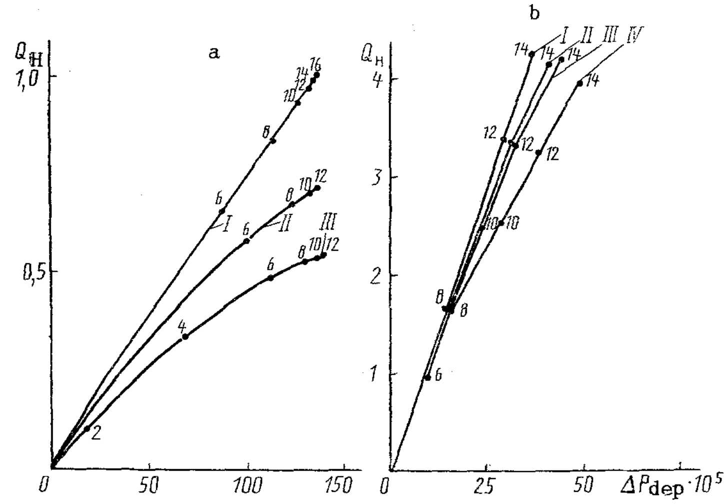

Fig. 2. Indicator curves: a) for a uniform bed: I) no degassing; II) $\Gamma_g = 250$ m^3/m^3, $\alpha = 0.01$, $P_{sat} = 23$ mPa; III) $\Gamma_g = 400$ m^3/m^3, $\alpha = 0.02$, $P_{sat} = 23$ MPa; b) for a nonuniform bed: I) no degassing; II) $\Gamma_g = 250$ m^3/m^3, $\alpha = 0.01$, $P_{sat} = 20$ MPa; III) $\Gamma_g = 250$ m^3/m^3; $\alpha = 0.01$, $P_{sat} = 23$ MPa; IV) $\Gamma_g = 400$ m^3/m^3, $\alpha = 0.02$, $P_{ast} = 23$ MPa. ΔP_{dep}, Pa; Q_{oil}, m^3/sec$\cdot 10^{-3}$.

Discussion of the Results of Numerical Simulation. In contrast to the model considered in [1], the present analysis is complemented with Eq. (10), derived from certain simplifying assumptions (quasistationarity condition) which makes it possible with an accuracy sufficient for the majority of practical problems to analyze the effect of bed degassing on the occurrence of more complex processes than those considered in [4].

In view of this, in addition to the 20-odd parameters involved in the system and given in [1], here such parameters appear as the oil saturation casing-head gas pressure P_{sat}, dynamic viscosities of gas μ_g and oil μ_{oil} under bed conditions, oil compressibility β_{oil}, casing-head gas solubility under bed conditions S, and gas number Γ_g typical of the given bed. Generally, all of these parameters depend on pressure in the form, for example, presented in [4]. For the proposed investigations these dependences can be replaced by certain constant values with regard to the range of their variation in real situations. Thus, usually, 6 MPa $\leq P_{sat} \leq P_b$; $0.01 \leq \alpha \leq 0.02$; $1 \leq S \leq 2$; $50 \leq \Gamma_{g0} \leq 600$ m^3/m^3; $1 \leq \beta_{oil} \leq 1.2$. Note that since the problem posed is solved numerically, the model allows one to take into account the characteristic form of these dependences on pressure for specific deposits. As already noted, the study will be carried out for the dependences of phase permeabilities on oil saturation as given by Eqs. (4).

Figure 2 presents the results of the study for the effect of degassing on indicator curves in the connecting pipe–well-bed model with the following parameters: *a*) $d_{con.p} = 6, 8, 10, 12, 14, 16$ mm ; $\bar{c} = 1.2$; $c_{oil} = 0.51$ kcal/(kg$\cdot$K); $\rho_{oil} = 800$ kg/m^3; $\rho_{g0} = 2$ kg/m^3; $\varepsilon = 0.4$; $P_2 = 2.0$ MPa; L = 2800 m; $2R_0 = 0.0685$ m. In case (a) the bed is assumed to be uniform, of thickness $H_b = 10$ m with the reservoir properties: $k = 10^{-14}$ m^2; cm $= 2\cdot 10^{-12}$ MPa^{-1}; $P_b = 23.0$ MPa; S = 10 m^3/MPa; $\beta_{oil} = 1$. In the other case, case (b), the bed is nonuniform: $H_2 = 4$ m; $H_3 = 1$ m; $H_4 = 5$ m; $k_2 = k_4 = 2\cdot 10^{-14}$ m^2; $k_3 = 10^{-12}$ m^2; $c_i m_i = 2\cdot 10^{-12}$ MPa^{-1} (i = 2, 3, 4).

Curve I in Fig. 2a corresponds to the case with degassing being absent in the bed (or when P_{sat} is very low) and is linear in the coordinates Q_{oil}, $\Delta P_{dep} = (P_b - P_s)$. The numerical values indicated at the points on the straight line correspond to the connecting pipe diameters for which the calculation was carried out. Everywhere, stationary values for Q_{oil} and P_s obtained after a lapse of 3600 sec were taken.

The deviation of curve II from curve I is due to the effect of degassing of the near-well zone of the bed. As the connecting pipe diameter becomes larger and the seam (and near-seam) pressure falls, the degassing-induced effect increases and at $d_{con} = 12$ mm attains almost 20%.

Indicator line III is even more nonlinear with an even greater effect of occurrence of nonlinearity with a rise in the connecting pipe diameter and in the discharge of the well.

The indicator curves for the above-described nonuniform bed (S = 10^3 m^3/MPa) are presented in Fig. 2b. At small values of $d_{con.p}$, curves I and II nearly coincide because the pressure in the bed everywhere exceeds $P_{sat} = 20$ MPa and there is no degassing of the oil.

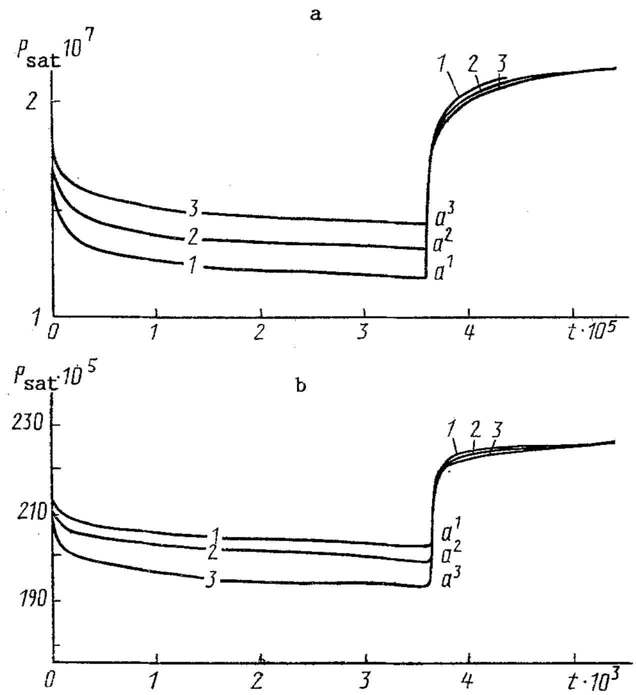

Fig. 3. The seam pressure P_s (Pa) vs time t (sec): a, for a uniform bed: 1) Γ_g = 400 m^3/m^3; α = 0.02; P_{sat} = 23 MPa; b) for a nonuniform bed: 1) Γ_g = 400 m^3/m^3; α = 0.02; P_{sat} = 23 MPa; 2) Γ_g = 250 m^3/m^3; α = 0.01; P_{sat} = 23 MPa; 3) no degassing.

As the connecting pipe diameter increases, the seam pressure falls and the nonlinear effect of bending of indicator curve II appears. When the saturation pressure $P_{sat} = P_b$ = 23 MPa (curve III), the degassing effect is observed in every part of the bed where $P(r, z, r) < P_{sat}$. The indicator curves obtained in this way are similar to those given in Fig. 3a. In this case (when the bed is nonuniform), the main distinctive features are: 1) since the effect of shunting by a highly permeable intercalated stratum results in a higher seam pressure, as compared with a uniform bed, the phase permeability coefficient for oil will be close to unity, and the degassing will exert a weaker effect on the form of the indicator curve; 2) since isolines are elongated (along the radius) due to the nonuniformity, the degassing zone will also have a noncylindrical shape, i.e., the degassing zone in a highly permeable intercalated stratum will be larger in radius than in weakly permeable blocks. On stoppage of the well, the observed effect reverses.

The dependences of the seam pressure P_s on time after putting the well into operation and its stoppage (KBD) for the connecting pipe of diameter $d_{con.p}$ = 6 mm and a uniform bed with $k = 10^{-14}$ m^2 are given in Fig. 3a. Curves 1, 2, and 3 correspond to the cases represented by curves I, II, and III in Fig. 2a. As is seen from Fig. 3a, the degassing effect is particularly pronounced in steady-state bed tests (the depressions are ΔP_d) and is barely perceptible in unsteady-state tests (the change in the fronts of the curves $P_s = P_s(t)$). This is attributable to the fact that during the fall of the seam pressure in the course of the start-up the overall degassing effect is very small, because a decrease in the phase permeability due to the degassing effect occurs in a small portion of the bed. At the stage of well stoppage the degassing effect is more noticeable, but is also small, since the seam pressure increases and the phase permeability tends to unity. The location of the points a^1, a^2, and a^3 that correspond to the seam pressures after the lapse of one hour differ greatly. All of these trends obtained on the model and observed in Figs. 2 and 3 are encountered in practice at all times and confirm the adequacy of the processes occurring in a real system and in a model. Setting the parameters of the model to actual deposits, it is possible, with the help of the solution of such straight problems, to quantitatively evaluate the effect of oil degassing in a bed and reduce to a minimum the errors in the interpretation of hydrodynamic tests of the beds and also to minimize the negative influence of oil degassing in the bed on the oil recovery coefficient.

Figure 3b presents the function $P_s = P_s(t)$ for a nonuniform bed with $d_{con.p} = 12$ mm. Degassing exerts a stronger effect on the results of steady-state tests (the magnitudes of depressions are much smaller than for a uniform bed at the points a^1, a^2, and a^3) and a weak effect on the results of nonsteady-state tests. The stoppage of the well is more sensitive to the effect of bed degassing than the start-up for the same reasons as in the case of a uniform bed.

As a result of the studies carried out, a number of conclusions can be drawn:

1. Oil degassing in a bed can significantly influence the results of hydrodynamic tests; it depends on such parameters of the bed fluid as the saturation pressure, gas solubility in oil, gas factor, viscosities of oil and gas, and oil compressibility. However, as a rule, the maximum effect does not exceed 30%.

2. The degassing effect is more influential in steady-state hydrodynamic tests.

3. Degassing in a bed leads to the appearance of a convex indicator curve of the bed; with an increase in the oil discharge (connecting pipe diameter) the deviation from the indicator curve without degassing increases.

4. The influence of degassing in a bed in hydrodynamic tests weakens in a nonuniform bed containing a highly permeable intercalated stratum (or cracks).

5. The effect of oil degassing in a bed should be analyzed in a system involving a connecting pipe and a well in which a gas–liquid mixture moves, since each of these elements produces its own effect, which is important for the general picture.

6. Since degassing has a weaker effect on the results of unsteady-state hydrodynamic tests, the latter provide a more suitable alternative for identification of the reservoir type. This especially refers to the well start-up curves.

7. All types of hydrodynamic tests of composite oil reservoirs should be conducted on a small-section connecting pipe (or at small discharges), since the influence of the effects associated with oil degassing the decreases.

8. In order to distinguish between the influence of oil degassing in a bed and mud grouting of cracks in the near-seam zone on the form of the indicator curve, it is necessary to carry out acid treatment of the bed. If the indicator curve remains intact, its deviation from a linear form can be assumed to be due to degassing; otherwise, due to the mud grouting of the near zone of the bed.

NOTATION

Here m_i is the bed porosity; $\bar{k}_i$, bed permeability; $\bar{k}_{oil} = k_{oil}/k$, $k_g = k_g/k$, relative phase permeabilities for oil and gas; ρ_{g0} and ρ_g, densities of gas under atmospheric and bed conditions; ρ_{oil0} and ρ_{oil}, oil densities under similar conditions; S, gas solubility in oil; μ_{oil} and μ_g, dynamic viscosities of oil and gas; β_{oil}, volumetric coefficient of oil; ω, cross-sectional area of bed; v_g and v_{oil}, filtration velocities of phases; C_i, bed compressibility; Q, volumetric flow rate of fluid; D, diameter of pipe (TS); G_g and G_{oil}, mass flow rates of gas and oil; φ, volumetric gas content; c_p and c_v, heat capacities of gas; c_{oil}, heat capacity of oil; $\varepsilon = G_g/(G_g + G_{oil})$, mass gas content; P_2, pressure downstream of connecting pipe; L, well depth.

LITERATURE CITED

1. S. D. Tseitlin and V. M. Il'inskii, Inzh.-Fiz. Zh., **59**, No. 4, 698-699 (1990).
2. K. S. Basniev, I. N. Vlasov, V. M. Kochina, et al., Underground Hydraulics [in Russian], Moscow (1986).
3. M. D. Rozenberg and S. A. Kundin, Filtration of Gasified Liquid and of Other Multicomponent Mixtures in Oil Beds [in Russian], Moscow (1969).
4. G. T. Bulgakov and G. A. Khalikov, Izv. Vyssh. Uchebn. Zaved., Neft' Gaz, No. 2, 49-53 (1980).
5. V. A. Evdokimova and I. N. Kochin, A Collection of Problems on Underground Hydraulics [in Russian], Moscow (1979).